JOURNAL OF MATERIALS SCIENCE 18 (1983) 1174–1182

Microstructure and mechanical properties of Al–$CuAl_2$ eutectic alloys solidified over a heat pipe

S. N. OJHA*, K. CHATTOPADHYAY†, P. RAMACHANDRARAO‡
Department of Metallurgical Engineering, Banaras Hindu University, Varanasi 221005, India

Microstructural studies and mechanical properties of Al–$CuAl_2$ eutectic alloys solidified over a heat pipe have been presented and discussed. The role of thermal undercooling produced by solidification over a heat pipe in controlling the microstructure has been highlighted. Tensile specimens fabricated from aligned cellular Al–$CuAl_2$ eutectic regions are shown to have maximum strength at intermediate temperatures of 450 to 500 K. Variations in the relative plasticity of two constituent phases of the eutectic are held responsible for the temperature dependence of strength.

1. Introduction

Heat pipe [1–4], as the name suggests, is a device of very high heat transfer capability. Coupled to a heat source at one end and sink at the other it can transport thermal energy over a considerable distance without an appreciable drop in temperature. Under ideal circumstances, this can have effective thermal conductivity orders of magnitude higher than that of pure copper [2, 4]. The possibility of exploitation of this device in solidification of molten metal was first discussed by Bahadori [5] and subsequently by Steininger and Reed [6]. However, their ideas were dormant until Chattopadhyay and Ramachandrarao [7] reported experimental investigations on the solidification of an Al–$CuAl_2$ eutectic over a heat pipe. In a later publication by Ojha *et al.* [8], a variety of microstructures were discussed in eutectic alloys solidified over a heat pipe. In regions nearest to the surface of the heat pipe, the casting exhibited a particulate morphology which is characteristic of a highly undercooled melt whereas in areas away from its surface a considerable alignment of eutectic cells was reported.

The present investigation was aimed at understanding the development of such particulate and cellular eutectic morphologies in the Al–$CuAl_2$ eutectic alloy and their influence on the mechanical behaviour of such composites. This alloy was chosen for investigation due to the availability of data regarding the influence of a range of cooling rates on its cast microstructures [9–11] and related mechanical properties [12, 13].

1.1. What is a heat pipe?

The heat pipe is basically a partially evacuated hollow container closed at both ends, containing a small quantity of working fluid which saturates a fine porous structure laid along the inner wall of the container (Fig. 1). Heat transfer by this device is effected by the cycle: evaporation of the working fluid → vapour transport → condensation of the vapour and recycling of the fluid by the capillary action of the porous structure. Consequently it is evident that a heat pipe can be divided into three main components along its axis. These include an evaporator, adiabatic and condenser sections. Through the evaporator

*Present address: Research and Development Centre, Steel Authority of India Ltd, Ranchi, India.
†Present address: Department of Metallurgy and Materials Science, Carnegie-Mellon University, Pittsburgh, PA 15213, USA.
‡Present address: School of Materials Science, Banaras Hindu University, Varanasi, India.

0022–2461/83 $03.00 + .12

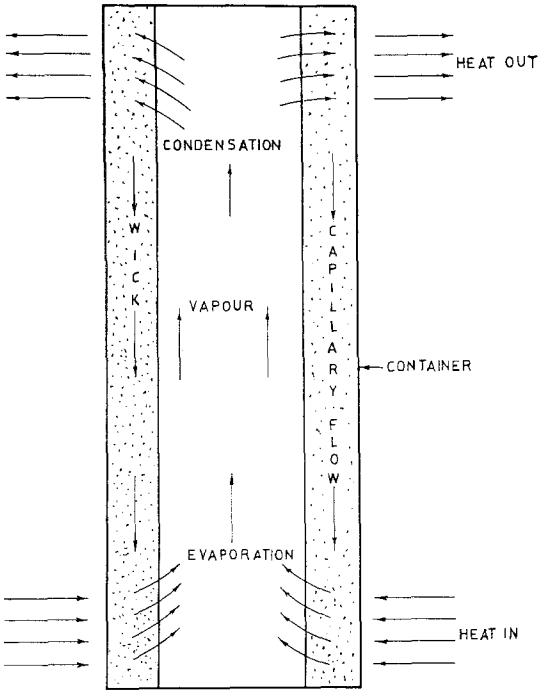

Figure 1 Schematic diagram of a heat pipe.

section, thermal energy from an external source is introduced into container walls and subsequently to the working fluid. In the condenser section the vapour of the working fluid condenses. The latent heat of condensation is dissipated to the surroundings by an appropriate cooling arrangement. These two sections are separated by an adiabatic section which provides passage for the movement of fluid and vapour between the above mentioned two sections. Since the heat transfer in a heat pipe is due to the vapour–fluid transport cycle, a definite quantity of heat is initially necessary for the initiation of this cycle. Thus heat pipes are generally preactivated before utilizing them for any experiment involving heat transfer. Excellent reviews [2–4] are available detailing the principle, construction and operation of a heat pipe.

2. Experimental work

In the present investigation a commercial heat pipe supplied by Noren Products Inc., California, USA was used which is capable of transferring heat fluxes of the order of 38 kW. Both commercial (99.95%) and high purity (99.999%) consistuent metals are used in preparing the Al–$CuAl_2$ eutectic alloys (17.3 at% copper) used in the present work. Details of the casting assembly have been shown in Fig. 2. The heat pipe and furnace were held on a stand in such a

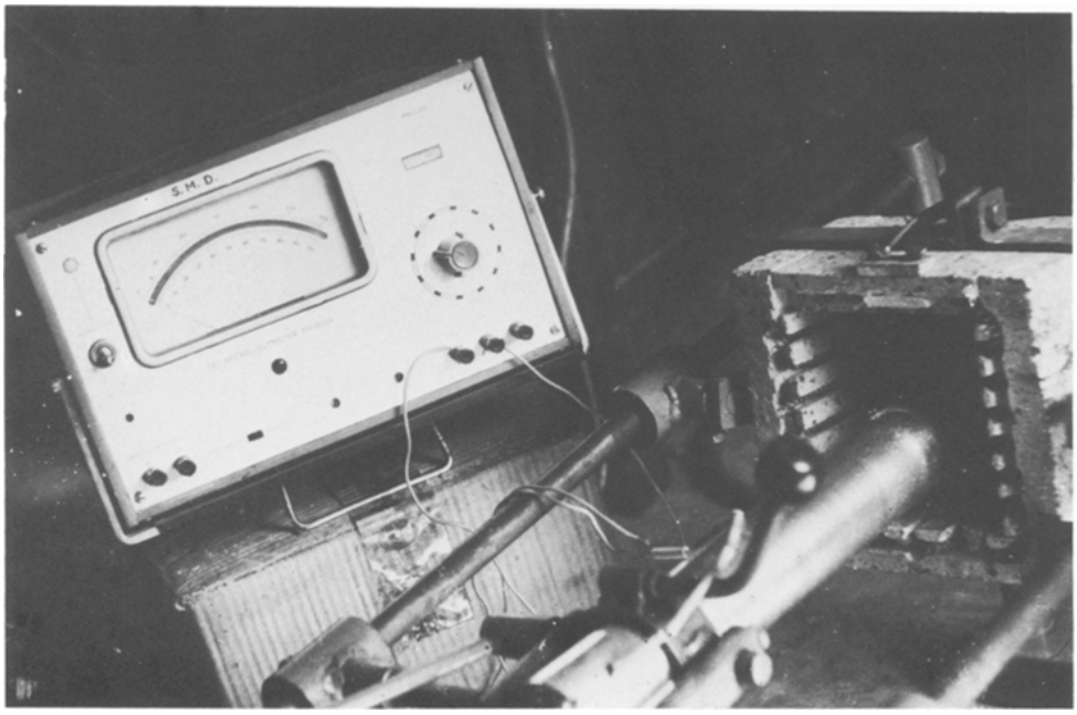

Figure 2 Experimental set-up for heat pipe solidification.

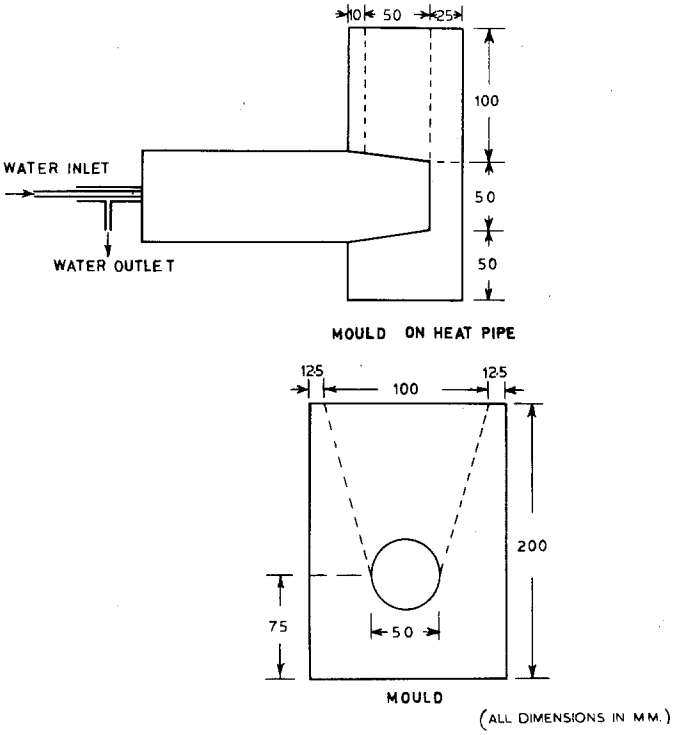

Figure 3 Diagram illustrating the heat pipe/mould assembly.

way that they could be tilted at any angle and moved apart to a considerable distance. The furnace in the assembly was designed and built specially to supply heat at the evaporator end of the heat pipe in order to activate it before casting the melt. Preactivation of the heat pipe was continued until the temperature at its condenser end reaches 373 K. The temperature at the condenser end was monitored using a sensitive microvoltmeter which recorded the output of a fine gauge chromel–alumel thermocouple inserted in the condenser end. The melt was cast in a refractory mould (Fig. 3) fitted to the evaporator section of the heat pipe, after starting circulation of water at the condenser end of the preactivated heat pipe. The total quantity of melt poured in each run was sufficient to almost completely fill the mould (about 10 cm x 5 cm x 10 cm). The castings were stripped between 40 to 60 sec after the hot metal was poured.

Transverse and longitudinal sections of castings were polished for metallographic examinations using standard procedures and examined in a Leitz metallograph. As discussed in the following sections, eutectic cells were aligned up to a considerable distance in the casting. Standard tensile specimens were fabricated from these regions of the castings such that cells are parallel to the tensile axis and tested in an Instron Testing Machine equipped with high temperature testing facility at a crosshead speed of 0.01 cm min^{-1}. Both the fracture surface as well as the longitudinal sections near the fractured region were examined in a Philips PSEM 500 scanning electron microscope.

3. Results and discussion

3.1. Microstructure of the Al–$CuAl_2$ eutectic solidified over the heat pipe

Under equilibrium solidification conditions the microstructure of Al–$CuAl_2$ eutectic has a lamellar morphology [14]. When this eutectic was solidified over a heat pipe interesting changes in microstructures could be observed. Similar results were obtained in both the commercial purity as well as high purity alloys. Fig. 4a shows the microstructure of the alloy solidified in contact with the surface of the heat pipe. A fine particulate morphology replaces the lamellar eutectic microstructure. This morphology was noticeable up to a distance of about 4 mm from the heat pipe surface. The average size of the particulate phase was found to vary from 5 to 10 μm depending on distance from heat pipe, the finer particles being closer to its surface. In some regions of the casting near the contact surface of the heat pipe

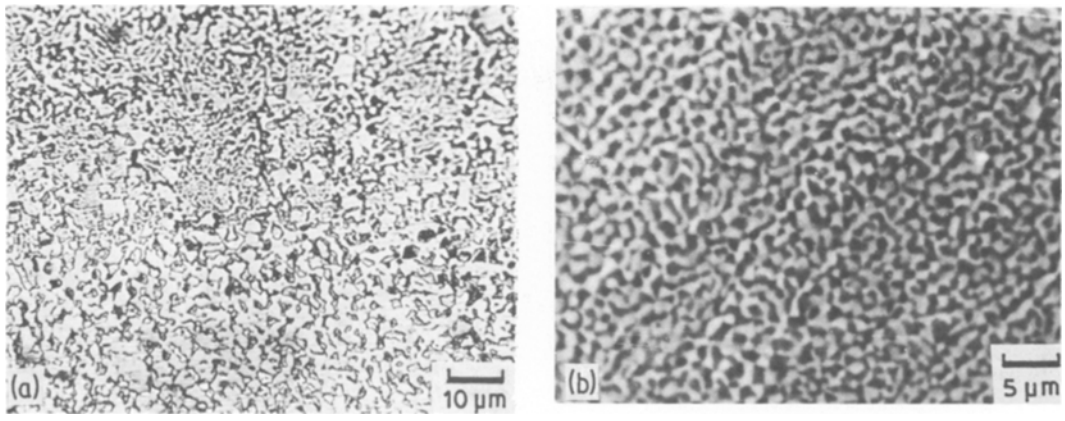

Figure 4 (a) Particulate eutectic morphology in an Al–$CuAl_2$ eutectic alloy solidified in contact with the heat pipe surface. (b) Degenerate eutectic microstructure.

a fine degenerate eutectic morphology (Fig. 4b) was also evident.

It is obvious from the above micrographs that in the immediate vicinity of the surface of the heat pipe, there is no tendency for eutectic cell formation. However, beyond 4 to 6 mm from the heat pipe surface, development of aligned cellular eutectic was noticeable (Figs. 5a and b). Initially, a number of cells nucleate and there appears to be competitive growth among them. At a later stage, more favourable cells grow in an aligned fashion with no further nucleation of cells. This aligned cellular morphology of the eutectic was observed to extend up to 3 to 5 cm in the casting.

At distances further away from heat pipe surface, the cells tend to branch resulting in eutectic dendritic morphology (Fig. 6). Even in these regions considerable alignment of the dendrites can be observed and the secondary arms gradually tend to align themselves parallel to the primary arms in the direction of the heat flow. Due to this tendency during growth the dendrites reveal a typical feathery morphology.

3.2. Estimation of cooling rate from microstructure

The cell spacing of Al–$CuAl_2$ eutectic alloy has been experimentally shown to be a function of the local freezing rate, given by the following expression [15]

$$c = 15.5(\mathrm{d}fs/\mathrm{d}t)^{-1/2} \quad (1)$$

where c is the cell spacing expressed in micrometres, fs is the fraction solidified and t is the local time in seconds. $\mathrm{d}fs/\mathrm{d}t$ represents the local freezing rate. Under the condition of Newtonian cooling, the cell spacing can be related through this relation to the local cooling rate $\dot{T}$ by the

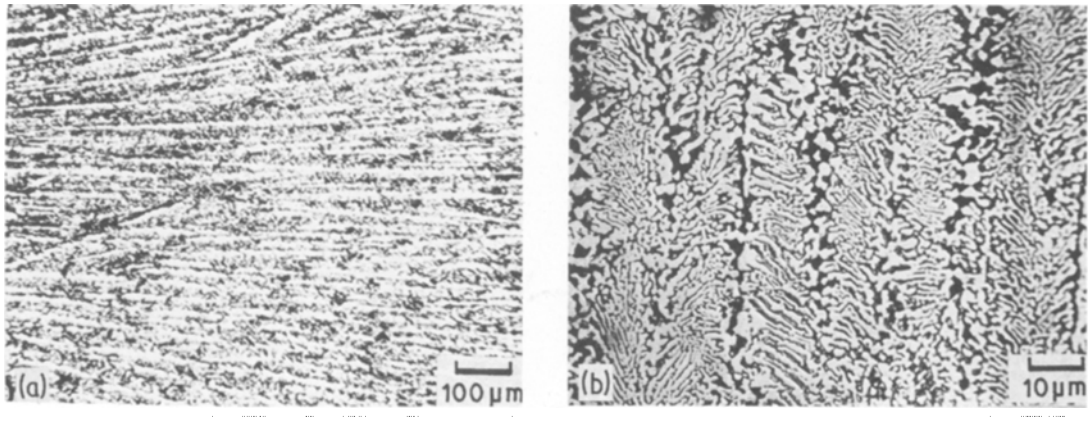

Figure 5 (a) Aligned cellular eutectic morphology in Al–$CuAl_2$ eutectic. (b) Aligned cellular eutectic morphology showing the orientation of lamellae inside cells of Fig. 5a.

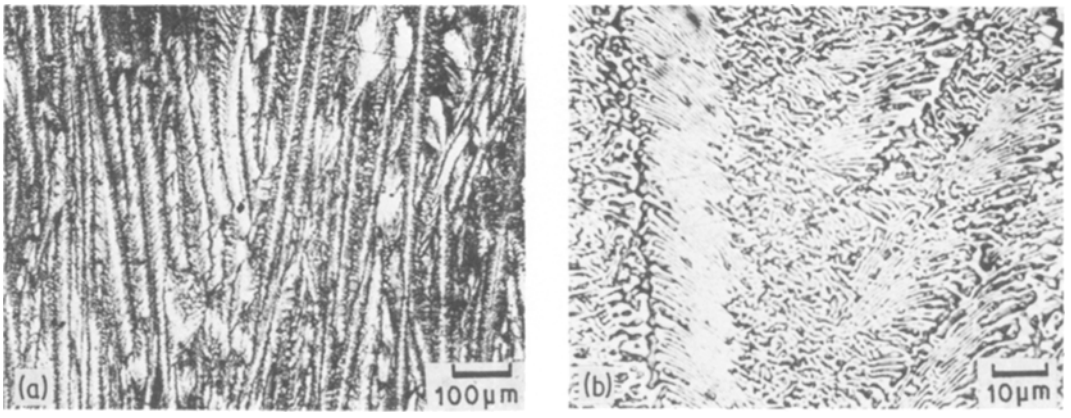

Figure 6 (a) Eutectic dendrites in Al–$CuAl_2$ eutectic solidified over a heat pipe. (b) Eutectic dendrites showing orientation of lamellae in primary stem and secondary branches of Fig. 6a.

following expression [16]:

$$\dot{T} = (15.5)^2 \frac{\Delta H^f}{c^2 \cdot C_p} \quad (2)$$

where ΔH^f is latent heat of fusion and C_p is the specific heat. For Al–$CuAl_2$ eutectic $\Delta H^f = 342\,kJ\,kg^{-1}$ and $C_p = 710\,J\,kg^{-1}\,K^{-1}$. Substituting these values the cooling rate becomes

$$\dot{T} = 1.157 \times 10^5 \times \frac{1}{c^2} \quad (3)$$

In Table I we have presented the overall cell size at different distances of our casting. The cooling rate calculated on the basis of the Equation 3 as a function of distance has been plotted in Fig. 7. However, the Nusselt number also will increase continuously away from the heat pipe surface. This will lead to an increasing departure from the Newtonian cooling condition. Thus the cooling rates in Fig. 7 represent only an upper bound of the prevailing cooling rates and the actual cooling rate near the top of the casting (for very high Nusselt number) can be less by an order of magnitude.

TABLE I Cooling rate distribution in the heat pipe cast specimens

Distance from heat pipe surface (mm)	Cell spacing (μm)	Cooling rate (assuming Newtonian cooling) ($ksec^{-1}$)
4	16.5	425
10	12.1	350
18	22.3	232
25	30	128

3.3. The origin of uncoupled eutectic

The consistent observation of a nonlamellar two phase structure in both the purity and commercial purity alloys indicate the existence of a special solidification condition near the heat pipe surface. Degenerate eutectics in Al–Cu system have been reported under the condition of extremely rapid [17] or extremely slow [18] cooling. The scale of the microstructure observed in the former case is much finer than the present case while we are further away from the latter condition. The two factors most probably responsible for the growth of this type of microstructure in the

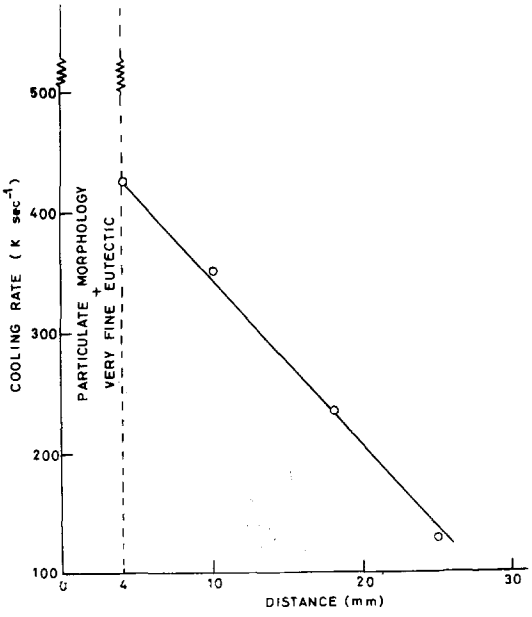

Figure 7 Variation of cooling rate in casting sections solidified over the heat pipe.

present case are the isothermal temperature of the heat sink and the prevailing undercooling. There are at least four models existing in the literature which try to explain similar morphologies. Uncoupled growth of the two phases of eutectic can take place due to changes in the relative velocities of the two phases on undercooling [19] or due to frequently branching two phase dendrites [20]. On the other hand a particulate type of morphology can also arise due to repeated nucleation of the second phase in the supercooled melt ahead of the primary phase [21] or due to the growth of a single phase of eutectic composition and its subsequent decomposition [22]. However, the last two mechanisms will yield probably much finer microstructure than the one observed by us. Further work is clearly necessary to determine the mechanism of the growth of our observed morphology.

3.4. Growth of eutectic cells and dendrites

The eutectic grows as cells due to instability of the planar solid/liquid interface arising either from constitutional undercooling ahead of solid/liquid interface due to rejection of impurities [23] or thermal undercooling due to high freezing rate [15, 24]. Formation of cells in Al–$CuAl_2$ eutectic has also been reported earlier [25] and cell size was found to be dependent upon both the growth rate and temperature gradients. Rohatgi and Adams [15] noticed such growth morphology on the surface of chill cast plates of Al–$CuAl_2$ eutectic. These investigators suggested that at high freezing rates the eutectic prefers to grow in the form of cylindrical cells while a decrease in freezing rate favours branching of cells and leads to the formation of eutectic dendrites. A fine lamellar eutectic was arranged in the form of dendrites with side branches and a coarse irregular eutectic was present in the interdendritic regions.

In contrast, Cantor and Chadwick [24] found the formation of eutectic dendrites at very high freezing rates which gradually transformed to cells with a decrease in freezing rate. The result was explained in terms of instability of the planar solid–liquid interface as a result of thermal undercooling induced by high freezing rate.

In the present experiments, once a solid layer forms on the contact surface of the heat pipe it offers resistance for heat transfer from the remaining melt. Thus, a continuous decrease in cooling rate of the melt can be expected at increasing distance in the melt from the surface of the heat pipe. Cooling rates as derived earlier from cellular spacings confirm this. Thus, the results of the present investigation are in agree-

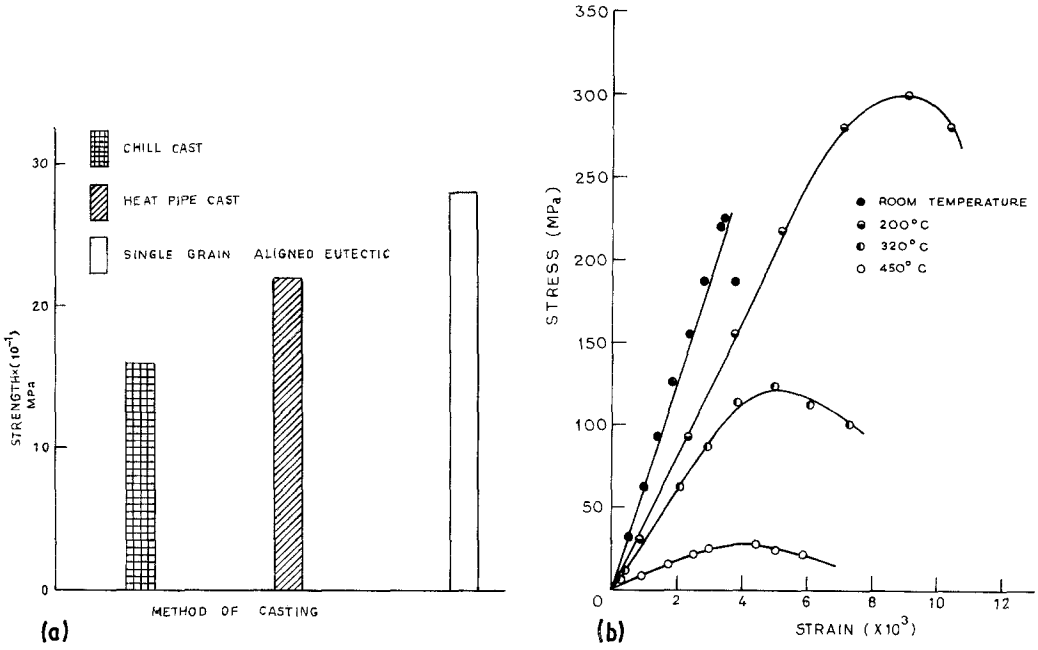

Figure 8 (a) Strength of Al–$CuAl_2$ eutectic cast under different conditions. (b) Engineering stress–strain plots for Al–$CuAl_2$ cellular eutectic.

TABLE II The mechanical properties of the heat pipe cast aligned cellular eutectic

Temperature (K)	UTS (MPa)	YS (MPa)	% elongation
300	220	–	3.5
473	300	252	17
593	120	112	35
723	27	24	29

ment with those of Rohatgi and Adams [15] since the eutectic dendrites were formed at the later stages of solidification.

3.5. The mechanical properties of the aligned cellular eutectic

The tensile tests have been carried out at different temperatures to evaulate the strength of the heat pipe cast Al–$CuAl_2$ cellular eutectic. In all these experiments the tensile axis is kept parallel to the cell growth direction. Fig. 8a shows a comparison of the ultimate tensile strength obtained on a steel mould cast, heat pipe cast and unidirectionally solidified Al–$CuAl_2$ eutectic alloys. The latter data has been taken from the work of Cantor and Chadwick [13]. Table II summarizes the strength data at various temperatures obtained by us. The corresponding stress–strain plots are presented in Fig. 8b. Jabezynski and Cantor [26] have earlier investigated the strength of aligned cellular chill cast Al–$CuAl_2$ eutectics where the growth rate varies with the length of the casting, and compared their results with those of Lawson and Kerr [27]. These latter investigators used a set-up where the cellular solidification takes place under a controlled steady state condition. Both the room temperature strength and work hardening rate obtained in the present investigation are very similar to those reported by Jabezynski and Cantor, and hence corroborate their findings.

One of the important findings of the present investigation is the nature of the temperature dependence of the UTS (ultimate tensile strength). The UTS value increases initially with a peak at 473 K before decreasing with temperature. However, the ductility increases continuously as reflected in the per cent elongation. The highest strength reached is close to that obtained by Cantor and Chadwick [13] for an aligned eutectic at room temperature. In Table III we have summarized the available high temperature data from the earlier works for comparison with our present results. None of the earlier data exhibits the present trend. It is believed that the reasons for such a behaviour can be traced to the nature of the fracture processes in relation to the cellular microstructure. Hence scanning electron microscopic observations were made on fracture surfaces as well as on the polished longitudinal sections close to the fracture surface. The failure at room temperature is by cleavage fracture (Fig. 9a) consistent with results of earlier investigations. However, at 473 K one observes small dimples in between $CuAl_2$ plates giving rise to a ductile fracture surface (Fig. 9b). At temperatures beyond this, the failure of both $CuAl_2$ platelets and matrix occur by a ductile mode. The observation of the longitudinal sections at room temperature indicate the fracture occurs by the nucleation of crack at the particle–matrix interface on the cell boundary and its subsequent propagation through the cell. At 473 K the cracks still nucleate at the cell boundary. But the enhanced ducility of the matrix inhibits their growth and results in the avoidance of premature fracture. At the same time the loadbearing capacity of $CuAl_2$ lamellae at this temperature is not affected [28]. Thus the strength of the composite increases and approaches that of unidirectionally aligned single crystal eutectic. Subsequent decrease at higher temperatures is due to loss of strength of both the matrix and $CuAl_2$ lamellae. The above results clearly demonstrate that under certain conditions, the cellular eutectic may have potential to perform as well as the aligned eutectic from the point of view of mechanical strength.

TABLE III Comparison of the high temperature strength data of the aligned Al–$CuAl_2$ eutectics obtained in earlier investigations with the present investigation

Temperature (K)	Ultimate tensile strength		
	Crossman *et al.* [12] (MPa)	Cantor and Chadwick [13] (MPa)	Present work (MPa)
RT (303)	169	280	220
423	145	–	–
473	–	–	300
523	76	–	–
593	34.5	159	120
723	–	46	27

4. Conclusions

The present investigation indicates that a variety of microstructures can be produced in an Al–

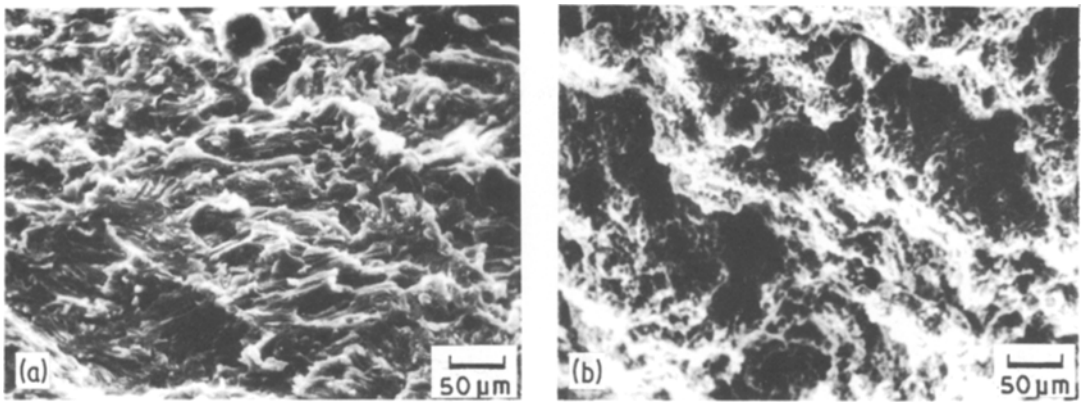

Figure 9 (a) Scanning electron micrograph showing cleavage fracture of cellular Al–$CuAl_2$ eutectic at room temperature. (b) SEM micrograph showing dimples in the matrix in Al–$CuAl_2$ cellular eutectic tested at 473 K.

$CuAl_2$ eutectic alloy solidified over a heat pipe. From the surface of the heat pipe to a distance of about 4 mm in the cast section, a 5 to 10 μm fine particulate morphology of the eutectic was noticeable. This particulate region is followed by cellular and dendritic growth morphologies of the eutectic.

The origin of these morphologies and other microstructural features can be explained on the basis of thermal undercooling induced in the melt as a result of rapid heat transfer capability of the heat pipe. The undercooling induced in the melt results in instability of the solid–liquid interface giving rise to various cast microstructure in the alloy.

The aligned cellular eutectic shows improved high temperature strength. The tensile specimens tested at 473, 593 and 723 K besides room temperature indicates a maximum strength at 473 K. Fractograph analysis revealed that the higher strength at 473 K is due to enhanced plasticity of the matrix which inhibits growth of cracks by yielding locally.

The enhancement in strength in the casting solidified over a heat pipe makes it a very promising device for commercial exploitation in the area of casting of metals and alloys.

Acknowledgements

The authors acknowledge the University Grant Commission, New Delhi for financial support and Professor R. W. Cahn, University of Sussex, Brighton, UK for providing the commercial heat pipe used in the present investigation. The authors are also grateful to Professor T. R. Anantharaman for encouragement.

References

1. G. M. GROVER, *J. Appl. Phys.* **35** (1964) 1990.
2. E. R. F. WINTER and W. O. BARSCH, "Advances in Heat Transfer", edited by T. R. Irvine, Jr and J. P. Hartnelt (Academic Press, New York, 1971) p. 219.
3. D. CHISOLM, "The Heat Pipes" (Pergamon Press, New York, 1976) p. 88.
4. P. D. DUNN and D. A. REAY, "Heat Pipes" 2nd edn (Pergamon Press, New York, 1978) p. 257.
5. M. N. BAHADORI, *Cast Met. Res. J.* **7** (1971) 62.
6. J. STEININGER and T. B. REED, *J. Cryst. Growth* **13/14** (1972) 106.
7. K. CHATTOPADHYAY and P. RAMACHANDRARAO, *Scripta Met.* 8 (1974) 1083.
8. S. N. OJHA, K. CHATTOPADHYAY and P. RAMACHANDRARAO, "Rapidly Quenched Metals III", edited by B. Cantor (The Metal Society, London, 1978) p. 119.
9. G. A. CHADWICK, *J. Inst. Met.* **19** (1963) 169.
10. R. W. KRAFT, *Trans. Met. Soc. AIME* **224** (1962) 65.
11. C. JANSEN, B. C. GIESSEN and N. J. GRANT, *J. Met.* **20** (1968) 91A.
12. F. W. CROSSMAN, A. S. YUE and A. E. VIDOZ, *Trans. Met. Soc. AIME* **245** (1969) 397.
13. B. CANTOR and G. A. CHADWICK, "Practical Metallic Composites" (The Institute of Metallurgists, London, 1974) D35.
14. R. W. KRAFT and D. L. ALBRIGHT, *Trans. Met. Sco. AIME* **221** (1961) 95.
15. P. K. ROHATGI and C. M. ADAMS, *Trans. Met. Soc. AIME* **245** (1969) 1609.
16. K. CHATTOPADHYAY, A. P. RAMINENI and P. RAMACHANDRARAO, *J. Mater. Sci.* **15** (1979) 797.
17. M. H. BURDEN and H. JONES, *J. Inst. Met.* **98** (1970) 249.
18. G. A. CHADWICK, *Prog. Mater. Sci.* **12** (1963–64) 142.
19. B. L. JONES, *Met. Trans.* **2** (1971) 2950.
20. M. F. CHELL and H. W. KERR, *ibid.* **3** (1972)

2002.
21. W. A. TILLER, "Liquid Metals and Solidification" (American Society for Metals, Cleveland, 1957) 276.
22. T. Z. KATTAMIS and M. C. FLEMINGS, *Met. Trans.* **1** (1970) 1449.
23. J. E. GRUZLESKI and W. C. WINEGARD, *J. Inst. Met.* **96** (1968) 304.
24. B. CANTOR and G. A. CHADWICK, *J. Mater. Sci.* **8** (1973) 830.
25. H. W. WEART and D. J. MACK, *Trans. Met. Soc. AIME* **212** (1958) 664.
26. F. S. J. JABEZYNSKI and B. CANTOR, *J. Mater. Sci.* **16** (1981) 2269.
27. W. H. S. LAWSON and H. W. KERR, *Met. Trans.* **2** (1971) 2853.
28. E. M. SAVITSKY, "The Influence of Temperature on the Mechanical Properties of Metals and Alloy" (Stanford University Press, Stanford, 1961) p. 165.

Received 16 April
and accepted 7 September 1982